Korean J. Chem. Eng., 34(10), 2703-2709 (2017)
DOI: 10.1007/s11814-017-0189-8

pISSN: 0256-1115
eISSN: 1975-7220

Influence of ethanol as bore fluid component on the morphological structure and performance of PES hollow fiber membrane for oil in water separation

Tunmise Ayode Otitoju, Abdul Latif Ahmad†, and Boon Seng Ooi

School of Chemical Engineering, Engineering Campus, Universiti Sains Malaysia, 14300, Nibong Tebal, Penang, Malaysia
(*Received 5 January 2017 • accepted 3 July 2017*)

Abstract−The relationships among varying bore fluid compositions containing ethanol/water were studied. The ethanol composition was varied in the ratio of 0%, 25%, 50%, 75% and 100%. The membrane dope solutions were prepared from 17.25 wt% polyethersulfone (PES), 0.75 wt% polyethylene glycol (PEG), 3 wt% silicon dioxide sol and 78.25 wt% of 1-methyl-2-pyrrolidone (NMP) via dry-jet spinning process. The membranes' morphology as a result of varying ethanol ratio in the bore fluid composition was characterized and their effects on crude oil/water emulsion separation were evaluated. Results show that the membrane pore size and porosity decreased with increasing ethanol content in the bore fluid mixture, whereas the inner wall thickness of fibers increased. Furthermore, an increase in ethanol concentration also resulted in a slight increase in water contact angle. The use of 100/0 of ethanol/water resulted in UF membranes with the lowest performance. On the other hand, bore fluid mixture containing 25/75 ethanol/water produced membrane with the best performance for crude oil/water separation. Overall, the use of bore fluid mixture containing 25/75 ethanol/water mixture was found to be a powerful way to tune the morphological properties and performance of HF membrane.

Keywords: Hollow Fiber Membrane, Bore Fluid, Ethanol, Polyethersulfone, Oil in Water Separation

INTRODUCTION

Membrane process refers to one of the most useful tools to introduce innovative approaches in pursuing goals such as process augmentation, reduction in production costs and low environmental impact [1-5]. Generally, membrane processes entail the use of a membrane with well-defined properties and performance. However, the knowledge of the material properties and the preparation processes of the membrane is of fundamental importance. In membrane processes, significant properties are hydrophilic/hydrophobic ability, mechanical and thermal stability and chemical resistance to alkali, acids and solvents [6].

The hollow fiber (HF) membrane configuration has been widely investigated as compared to flat sheet membrane configuration, due to its outstanding characteristics such as high surface area to volume ratio of module, higher productivity per unit volume, mechanically self-supporting and their good flexibility in operation [7-9]. In hollow fiber membrane configuration, the important membrane preparation methods are all based on the phase inversion process such as dry-wet spinning, melt spinning and dry spinning [10]. Different parameters, including the polymer concentration, solvent type, flow rate of the dope solution and bore fluid, humidity as well as temperature of spinning environment have been found to play a vital role in the phase inversion process [11].

Efforts have recently been made to enhance the structural morphology and performance of HF membrane via changing the compositions and variation of spinning solution [12-16], air gap distance [17,18], coagulation bath and temperature [19], dope flow rates [20], bore fluids [21] and take-up speed (TS) [22]. Bore fluid composition is one important parameter that can affect the morphology and performance of the produced HF membrane. However, such an important role is generally ignored and only few investigations on the influence of bore fluids composition on the morphological evolution of the resultant HF membranes have been reported. Some studies have concluded that the selection of bore fluid components is vital, as the chosen bore fluid components must be able to provide an open lumen at the inner part of the HF membrane without endangering the phase inversion processes occurring at the outer surface of the membrane [23]. The composition and bore fluid type are of great importance for controlling membrane morphological properties [24], which can be caused by an exchange of solvent and non-solvent in the bore fluid. Many studies have shown that bore fluid exhibits a tendency to control the formation of the skin layers during spinning [23,25-28]. In a study by [29] stated that the pore size of inner surface can be affected by the bore fluid exchange rate. Generally, the influence of the bore fluids cannot be limited to the production of a standard lumen shape. The use of different bore fluids has been reported in the literature, each with varying effect on the fiber [6,30,31]. Based on experiences gathered from past studies, the use of gaseous bore fluids is unsuitable due to concerns over the ability to prevent oval bores caused by reduction in vitrification rates and the limitations to control the low gas pressure [32]. The addition of solvent such as NMP, DMAc and potassium acetate to the bore fluid component has been widely carried out in the past [33-38], sometimes leading to opposing conclusions. For polysulfone gas-separation membranes, [36] reported that the selectivity increased when the water activity was lower in the bore fluid, although they did not find any significant difference

†To whom correspondence should be addressed.
E-mail: chlatif@usm.my

in permeance and selectivity with membranes spun with DMAc/water mixture as bore fluid. Meanwhile, selectivity of the gas membranes showed a significant influence with potassium acetate/water mixture as bore fluid. For polysulfone ultrafiltration membranes, [33,39] found that the solute rejection decreased when they used bore fluids with reduced water activity.

The use of soft non-solvents such as ethanol has not been mentioned in the literature, and their influence on membrane properties and performance remains controversial. When ethanol fraction is added into water, the surface tension of water tends to reduce and can also provide a high degree of hydrogen bonding effects during the phase inversion. Although, there is no dispute that ethanol alters membrane properties, as assayed upon addition in bore fluid composition, but are these effects sufficient to alter membrane structure and performance? To address these questions, and to explore the morphological relationships and performance of membranes fabricated using ethanol with different concentration in the bore fluid mixtures, this study is necessitated. In addition, the intrinsic correlation between ethanol of varied composition in the bore fluid liquid may develop more understanding of their potential for industrial applications, which will be used as a guideline for membrane end users and also serve as a guide for membrane characterization in the future of membrane filtration.

The aim of this study was to gain more knowledge into the influence of ethanol variation in bore fluid composition on the membrane formation and performance of the resulting PES hollow fiber membrane. The PES HF membranes were successfully prepared via altering the bore fluid compositions with ethanol while other spinning parameters were maintained constant. To achieve the aforementioned objectives, five bore fluid mixtures were used by varying the composition of ethanol content in the ratio of 0%, 25%, 50%, 75% and 100%. The resulting membranes were characterized and their performance for crude oil in water emulsion was evaluated.

MATERIALS AND METHOD

1. Materials

Polyethersulfone (PES Ultrason E6020P) with molecular weight of 58,000 g/mol was kindly provided by BASF. Polyethylene glycol (MW is 35,000 Da) was purchased from Sigma Aldrich. Tetraethoxysilane (TEOS), ethanol and NMP were supplied by Merck, Malaysia. Nitrogen gas and liquid nitrogen were supplied by Wellgas, Malaysia. Crude oil was supplied by Petronas, Malaysia.

2. Synthesis of Silicon Dioxide Sol

The synthesis of silica sol followed a similar process as reported by [40]. Typically, silicon dioxide sol was prepared by adding TEOS (2.45 ml) and ethanol (1.45 ml) to a mixture of deionized water (1.45 ml) and acetic acid (0.4 ml) followed by stirring at ambient temperature for 5 h until a transparent sol is attained.

3. Membrane Preparation

The procedure for the membrane fabrication was as follows: PES was dried in oven at 75 °C for 3 h prior to use. 17.25 wt% PES, 1.75 wt% PEG and 3 wt% transparent silica sol were dissolved in 78 wt% NMP. The solution was continuously stirred at 60 °C for at least 15 h until a clear homogenous mix was achieved. Afterwards, the solution was de-aerated by leaving in the dark overnight until the bubbles were completely removed. The bubble-free solution was poured in the dope tank.

Table 1. Membrane samples according to bore fluid composition

Membrane code	Bore fluid components (wt%)
BF 1	Ethanol (0 wt%): distilled water (100 wt%)
BF 2	Ethanol (25 wt%): distilled water (75 wt%)
BF 3	Ethanol (50 wt%): distilled water (50 wt%)
BF 4	Ethanol (75 wt%): distilled water (25 wt%)
BF 5	Ethanol (100 wt%)): distilled water (0 wt%)

Table 2. Spinning conditions for hollow fiber membrane

Parameters	Values
Coagulation bath (°C)	25
Bore liquid flow rate (ml/min)	1.8
External coagulant	Pure water
Air gap (cm)	25.5
Spinneret internal diameter (mm)	0.50
Spinneret external diameter (mm)	1.00
Room temperature (°C)	21-22
Collection drum (rev/min)	7.998
Gear pump (rev/min)	18
Relative humidity	63-67

Hollow fiber membranes were produced via the dry/wet spinning process [41]. In this study, the bore liquid compositions were varied as shown in Table 1 while other spinning parameters were left constant throughout the whole fabrication processes. The spinning conditions that were maintained constant are summarized in Table 2.

The produced membranes were kept in water for 48 h while the water was concurrently changed to fully eliminate the left over solvent.

4. Field Emission Scanning Electron Microscopy (FESEM)

Prior to SEM analysis, the membrane pieces were thoroughly rinsed with distilled water, transferred to a glycerol/water (50/50) solution and then dried at room temperature. For the SEM morphological cross-sections analysis, the membrane samples were fractured via immersion in liquid nitrogen. For the case of the membrane surface, the samples were cut into small pieces and affixed horizontally on a double-sided adhesive foil which serves as the membrane sample holder. Before SEM imaging, sputter coating (Quorum - SC7620) was applied on the surface and cross sectional area of the samples to prevent from electrostatic discharge. Membrane cross-section and surfaces were observed via the Supra TM 35vp Zeiss.

5. Porosity and Pore Size

The porosity of membrane can be defined as the volume of pores per the total volume of the porous membrane and can be determined using the below Eq. (1):

$$\varepsilon = \frac{\frac{ww - wd}{dw}}{\frac{ww - wd}{dw} + \frac{wd}{dp}} \times 100 \quad (1)$$

where ε is the overall porosity (%), ww is the weight of the wet sam-

ple (g), wd is the weight of the dry sample (g), dp is density of PES polymer (1.36 g/cm^3) and dw is density of water (0.998 g/cm^3).

The mean pore size of all HF membranes was calculated from solute transport information. The concentrations of the solute (PEG) were obtained using total organic carbon (TOC) analyzer (TOC-VCPH total organic carbon analyzer-SHIMADZU).

6. Contact Angle Measurement

The contact angle (CA) was used to determine the surface hydrophilicity with a goniometer (Rame-Hart 250-F1, USA) at ambient temperature. The membranes were placed horizontally on a glass slide using double sided tape. A water droplet (0.5 μL) was placed on the dried membrane surface using a motor driven microsyringe at room temperature (21±1 °C). To reduce experimental error, five readings were taken at different locations on the membrane surface and their average CA values were calculated.

7. Fourier Transform Infrared Spectroscopy (FTIR)

The chemical composition of all HF membranes was characterized by using FTIR spectroscopy (FTIR Nicolet Nexus 670, USA) over a wave number range of 4,000-500 cm^{-1}. The membrane samples were affixed to a diamond crystal which was operated at 45° incidence angle. Individual spectrum was captured with an average of 32 scans at a resolution of 4 cm^{-1}.

8. Membrane Separation Performance Studies

8-1. Preparation of Oil in Water Separation

In oil in water emulsions, oil is dispersed as liquid droplets through the water which is in the continuous phase. These oil droplets generally tend to coalesce to form bigger drops. The smaller the droplets, the greater the surface tension, which implies that the force needed for merging will be greater; so, such emulsion is said to be stable in comparison to an emulsion containing larger oil droplets. As this study is associated with ultrafiltration (UF) of stable oil in water emulsion, we attempted to prepare samples of oily water containing smaller sized oil droplets (<5 μm). Crude oil was used without any treatment to prepare the emulsion. The oil in water solution (395 mg/L) was derived by mixing crude oil and de-ionized by stirring at 450 rpm speed over a period of 15 h until the solution was homogeneous and found stable (absence of oil layer on top of the solution). The size of the oil droplets was measured using a Malvern Mastersizer 2000. The oil concentrations in the feed and permeate were determined using a UV-visible spectrophotometer (Pharo 300) at a wavelength of 225 nm.

8-2. Ultrafiltration Experiment

The pure water flux (PWF), oil permeate flux (OPF) and oil rejection were determined by using cross flow filtration with active filtration area of 0.0080 m^2. The filtration rig consisted of the feed tank, peristaltic pump, pressure gauge, cross-flow cell, and control valve. Typically, the pump was used to transfer the feed from the feed tank at a flow rate of 400 ml/min. All experiments were under ambient temperature (22±1 °C). Four fibers with effective fiber length of 46.5 cm were attached to the module holder. Prior to ultrafiltration testing, the membrane samples were soaked in ethanol for at least 3 h. and then kept in distilled water for two days.

Prior to this process, compression tests were carried out for all membranes with distilled water at 2 bar for 3 h. Then, pure water flux (PWF) and oil permeate flux (OPF) measurement was determined at 1.5 bar, and the PWF and permeate flux was determined after 2 h of oil in water filtration.

The PWF and OPF were calculated using Eq. (2):

$$J_f = \frac{V}{A * t} \tag{2}$$

where J_f is PWF and OPF (L/m^{2}h), V is the permeate volume (L), A refers to the membrane surface area (m^2) and t refers to the measurement time (h).

The membrane oil rejection was determined by using Eq. (3):

$$R = \left(1 - \frac{X_p}{X_f}\right) \times 100 \tag{3}$$

where R (%), X_p (mg/L) and X_f (mg/L) represents oil rejection, oil concentrations in the permeate and feed, respectively.

8-3. Cleaning and Regeneration of Membranes

After a filtration test, the permeate flux of all the membranes tends to decline due to fouling. To regenerate membrane and resume the permeation flux of membranes as much as possible, it is necessary to remove pollutants by membrane cleaning. Membranes were cleaned by using DI water and 3 wt% NaOH solution for 30 min, respectively. This was to examine whether the permeate flux can be recovered as high as possible using the physical and chemical cleaning process. Hereafter, the stable permeation flux after membrane cleaning is denoted as J_c and calculated using Eq. (4):

$$J_c = \frac{V}{A * t} \tag{4}$$

To calculate the defouling property and the membrane cleaning efficiency, the flux recovery ratio (FRR) was calculated based on Eq. (5):

$$FRR = \left(\frac{J_c}{J_{pwf}}\right) \times 100 \tag{5}$$

J_c is pure water flux (after physical and chemical cleaning) (L/m^{2}h) and J_{pwf} is initial pure water flux (L/m^{2}h).

RESULTS AND DISCUSSION

1. SEM Analysis

FE-SEM was used to examine the surface and cross-sectional area of the produced membrane. Fig. 1 displays the FESEM images of prepared PES HF membranes. As shown, all spun membranes displayed fingerlike structure in their cross-sectional morphology. Generally, in the fabrication of HF membrane via phase inversion, the formation of finger-like macro-voids is often observed, due to the instantaneous liquid-liquid demixing during the coagulation process [42,43]. As shown in Fig. 1, BF 1 membrane displayed finger-like structure with large macrovoids in its sub-layer cavity, somewhat deeper while a better arrangement of the finger-like structure was better for BF 2. With ethanol concentration of 25 wt% in the bore fluid, the finger-like structures were more pronounced and regular. Furthermore, there were no visible macrovoids on the cross-section of BF 2 membrane. This can be attributed to the delay in the rate of precipitation at the inner layer of the nascent membrane, which causes suppression in the formation of finger-like as well as macrovoid pores [1]. As seen from the cross-

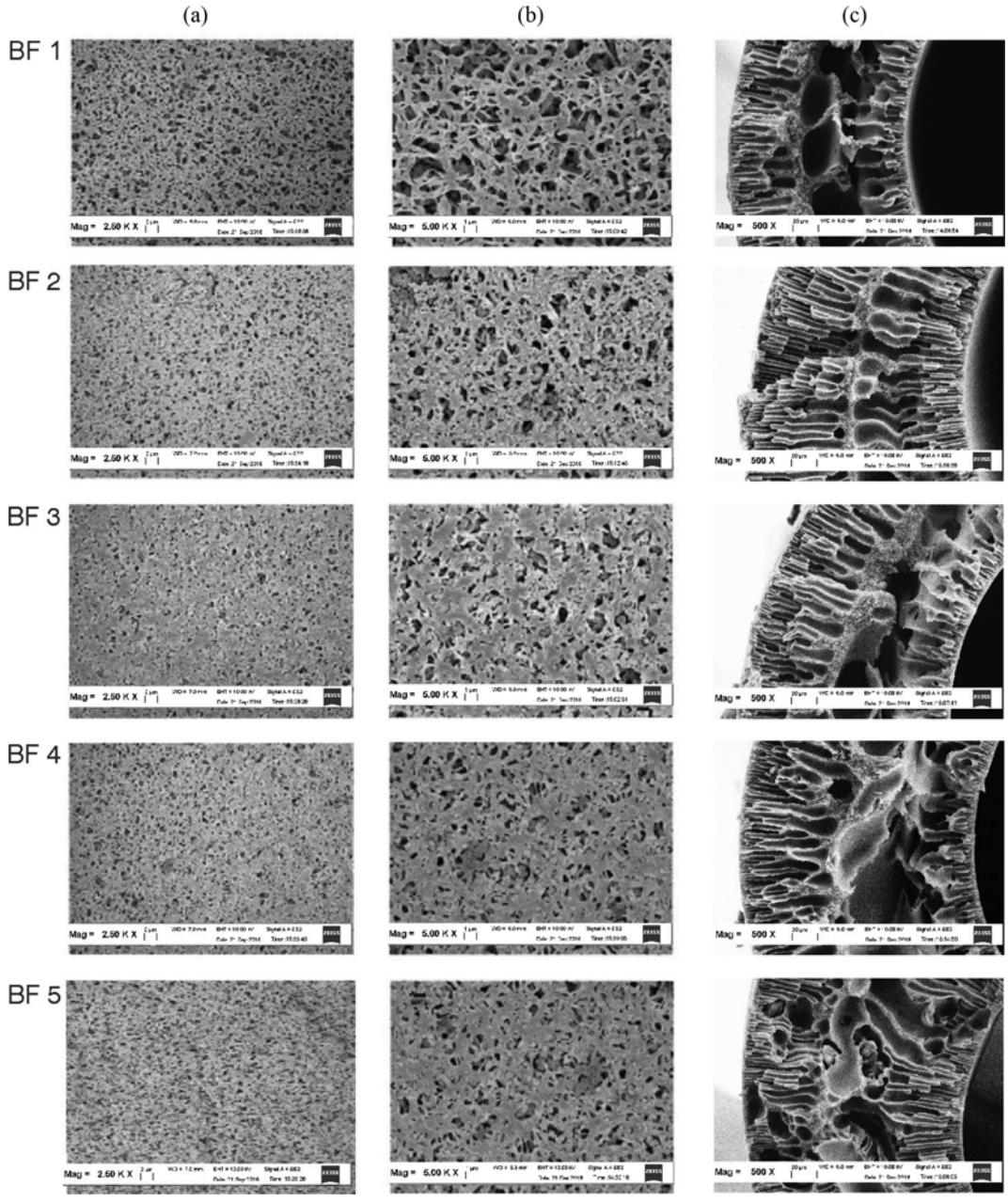

Fig. 1. FESEM micrographs of membranes. (a) Surface at 2.50 K X, (b) Surface at 5.00 K X, (c) Cross-section at 500 X.

section, irregularity exists in the arrangement of finger-lie structure of the membranes as ethanol concentration increases from 50 to 100% ratio. This can be caused by the decrease in diffusivity of the non-solvent, resulting to increase in time scale at which the entire process of phase inversion takes place, subsequently resulting in delaying the onset of demixing. Furthermore, macrovoid formation in the cross-sectional image also decreases with increase in ethanol concentration.

The internal wall thickness was measured and summarized in Table 3. As shown, the thickness of the membranes slightly increases with increase in ethanol concentration in the bore fluid composition. This is in good agreement with study by [33] for the PEEKWC UF membranes. Among all membranes, BF 5 membrane shows the highest internal wall thickness as compared to all other membranes. The thickness of the inner wall boundary on

Table 3. Effect of bore fluid composition on membrane porosity and pore size

Membrane code	Porosity (%)	Mean skin pore size (μm)	Inner wall thickness (mm)
BF 1	75.25	0.1545	0.79
BF 2	75.39	0.1383	1.18
BF 3	73.64	0.1187	1.32
BF 4	72.27	0.1117	1.49
BF 5	64.88	0.0933	1.58

the lumen side of BF 1 was measured to be ~0.80 mm, which is half the inner wall thickness of BF 5 membrane. This can be attributed mainly to the inflation of the fiber caused by the much higher flux of the bore fluid than that of the dope solution. However, bore fluid composition containing only distilled water will instantaneously create a rigid wall thickness that is difficult to inflate, while bore composition like the 50/50, 75/25 and 100/0 ethanol/water mixture leads to a delayed onset of liquid-liquid demixing and hence a slower gelation, thus allowing a stronger inflation of the fiber.

Comparing the surface of all membranes, there is a significant decrease in pore size with increase in ethanol concentration, which can be attributed to suppression in the coagulant phase. However, the pore size of membranes has a significant influence on permeation flux, which will discussed later.

2. Porosity and Pore Size Analysis

Table 3 presents the porosity and the mean pore size data of the prepared membranes. Porosity is between 64.88 to 75.39%. Effective surface porosity of membrane increased significantly by the addition of ethanol in bore fluid component.

Table 3 also shows the mean pore size of the produced HF membranes. All prepared membranes were found to be porous as can be seen in Fig. 1 and Table 3. Result shows that the pore size of all membrane in the skin layer decreases with increasing in ethanol content in the bore fluid mixture. This can be caused by suppression in the coagulant phase inversion with increasing in ethanol content, as the water and ethanol mixture diffused into the dope solution at a slower rate than when 100% water was present in the bore fluid. The introduced nuclei are susceptible to grow before the phase inversion process begins to take place as the longer the nuclei in the skin layer grows, the larger the pores become, as that is the case when 100% water was used as the bore fluid. This reason is in tandem with the slight decrease in contact angle and high permeate flux due to the high pore size of BF 1 membrane (Fig. 1 and Table 4). From these results, it is evident that the size of pores can be directly controlled by manipulating the amount of ethanol composition in the bore fluid mixture. The porosity of the all membranes decreases with increasing content of ethanol in the bore fluid composition with BF 2 membrane displaying the highest porosity.

3. Contact Angle Measurement

The influence of bore fluids mixtures on water contact angle is summarized in Fig. 2. As shown, BF 1 exhibited the lowest contact angle, which was lower than other membranes. It can be noticed that the water contact angle increased with increasing ethanol content in the bore fluid composition. When ethanol concentration was

Table 4. The influence of bore fluid compositions on permeate flux and rejection

Membrane code	Permeate flux (L/m^{2}h)	Rejection (%)
BF 1	79.81	97.85
BF 2	76.67	98.57
BF 3	73.01	97.32
BF 4	73.26	97.01
BF 5	69.65	95.32

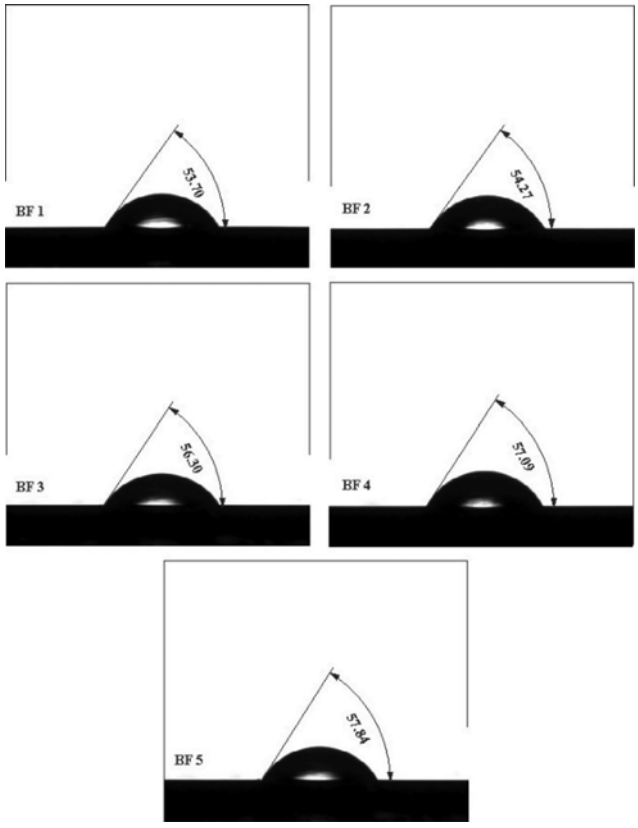

Fig. 2. Effects of bore fluid compositions on water contact angles.

100%, the water contact angle increased to 57.84°. The increase in contact angle with increasing ethanol concentration can be attributed to the decreasing trend of pore size of the membranes. The low contact angle of BF 1 membrane can be due to its higher pore size, which was responsible for the permeation flux (Table 4).

4. FTIR Analysis

FTIR test was used to assess the possible change in the PES HF

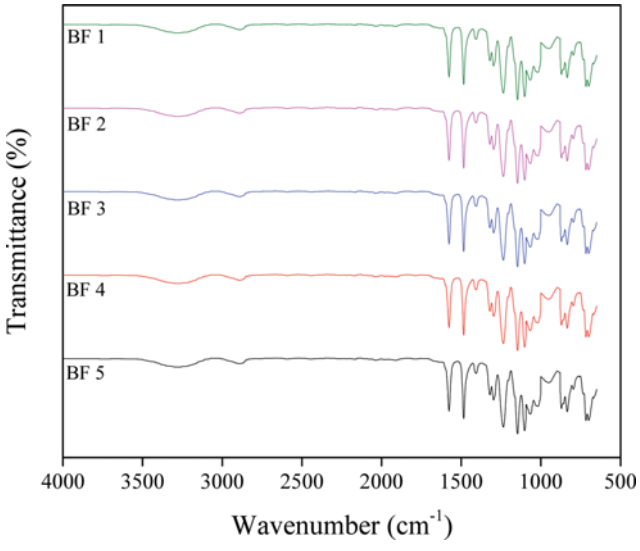

Fig. 3. FTIR spectra of BF 1, BF 2, BF 3, BF 4 and BF 5 membranes.

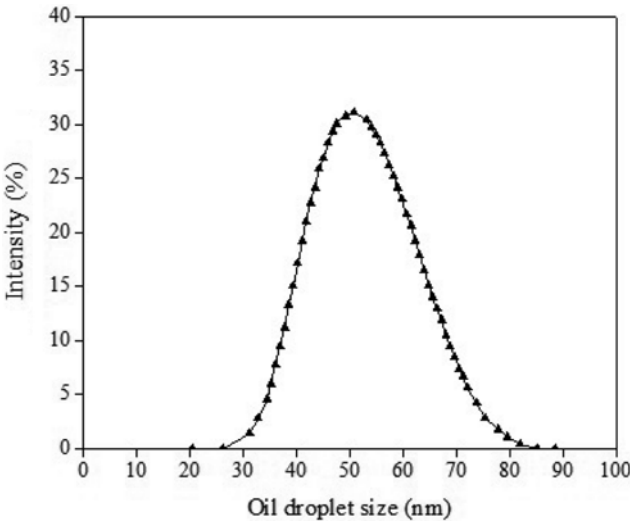

Fig. 4. The size distribution of oil droplet in the oil in water emulsion for the ultra-filtration separation.

chemical structure and functional groups due to chemical interaction upon the addition of varying composition of ethanol in the bore fluid mixtures. The FTIR spectra as shown in Fig. 3 did not reveal any significant difference between the membranes.

5. Membrane Separation Performance

The prepared membranes were used for ultrafiltration of the oil in water emulsion. The mean average particle size was ~0.056 μm (as shown in Fig. 4). Two experiments for each membrane were carried out and the average of individual fluxes was estimated. Table 4 shows the influence of bore fluid composition on permeate flux and rejection for crude oil in water emulsion filtration. However, among all prepared membranes, BF 2 membrane shows the highest rejection (98.57%) with moderate permeate flux (76.67 L/m^2h). The above performance seems to be related not only to the difference in the surface porosity but also variations in the pore size, which can aid the membrane to fast absorb water molecules. Furthermore, oil rejection increases with increases in ethanol concentration in the bore fluid.

6. Anti-fouling Performance of the Membranes

In the treatment of oil emulsion using membrane systems, the regeneration of the membranes is always an important issue as there is adsorption of solute on the membrane surface [44,45]. In oily wastewater treatment, two types of membrane fouling normally occur, which includes reversible and irreversible fouling. Both types of fouling can result to flux decline of the membrane. The former is generated by deposition of oil particles on the pores as well as on the surface of the membrane. In reversible fouling, the flux decline can be recovered by backwashing with pure water. The irreversible fouling is caused by physical/chemical sorption of oil particles in the pores and on membrane surface. In most cases, flux decline in irreversible fouling can be recovered by washing with basic or acidic solutions, but sometimes cannot be recovered even when aggressive cleaning methods are applied.

A higher FRR value represents a better anti-fouling property. A supplementary and comparative study was also conducted for the prepared membranes with oil/water separation. As shown in Table 5, the flux recovery of all membranes was good after washing with deionized water and 3 wt% NaOH aqueous solution. The optimum membrane (BF 2) membrane exhibits a better flux recovery than all prepared membrane, indicating a better antifouling property. This is because the BF 2 had a moderate pore size and porosity which as such will require a lower shear force while detaching the cake layer. Overall, this result confirms that the developed membrane using a mixture of 25/75 ethanol/water mixture has a significant influence on the performance improvement of the membrane. Besides, the membrane cleaning effects using 3 wt% NaOH aqueous solution were much superior to those using DI water.

Table 5. Flux recovery of fouled membranes after membrane cleaning

Membrane	DI water			3 wt% NaOH solution		
	J_{f1} (L/m^2h)	J_c (L/m^2h)	FRR (%)	J_{f2} (L/m^2h)	J_c (L/m^2h)	FRR (%)
BF 1	129	100	78	132	123	93
BF 2	117	95	81	116	110	95
BF 3	110	84	76	112	101	90
BF 4	101	71	70	107	89	83
BF 5	89	52	58	94	71	67

Operating condition: TMP=1.5 bar, flow rate=400 ml/min, temperature=25 °C, oil concentration=395 mg/L, ultrafiltration time=2 h, cleaning time=0.5 h

CONCLUSIONS

We investigated the influence of varying bore fluid composition. PES HF membranes were fabricated via dry/wet spinning process by varying the concentration of ethanol in the bore fluid composition. The prepared membranes were packed into membrane modules and tested for crude oil/water separation. Among all membranes, BF 2 membrane was found to be the optimum membrane, displaying a moderate pore size and high porosity. In addition, the pore size decreased with increase in ethanol concentration in the bore fluid concentration, whereas the porosity increased. An increase in ethanol concentration resulted to increase in internal wall thickness of the fibers, which was apparently a result of the variations on demixing rates. Furthermore, an increase in ethanol concentration also resulted in a slight increase in the membrane contact angle. The performance of BF 2 membrane for oil/water separation was found superior as compared to all other prepared membranes. Differences in membrane performance were related to the increments of pore size and porosity induced by the concentration of ethanol in the bore fluid. Although, the general problem was that all prepared membranes could not be fully regenerated by using conventional cleaning methods, as this is the common case for most prepared membrane when tested for oil/water emulsion. Moreover, the flux recovery of fouled BF 2 membrane was much more superior as compared to all fouled membrane. Considering the performance, experimental data of all membrane, it can be concluded that by using a mixture of 25/75 ethanol/water mixture, membranes with desirable membrane structure and perfor-

mance for crude oil in water emulsion can be achieved.

ACKNOWLEDGEMENTS

The authors acknowledge the financial support provided by Universiti Sains Malaysia under the USM fellowship scheme, Fundamental Research Grant Scheme (FRGS), Long Term Research Grant Scheme (LRGS), Ministry of Higher Education (MOHE) Malaysia (Grant no: 203/PJKIMIA/6071334 and 203.PJKIMIA.6726101), and Universiti Sains Malaysia (USM) RU Membrane Science and Technology Cluster.

REFERENCES

1. R. Saghafi, M. Zarrebini, D. Semnani and M. Mahmoudi, *Text. Res. J.*, **85**, 281 (2014).
2. A. L. Ahmad, A. A. Abdulkarim, S. Ismail and O. B. Seng, *Korean J. Chem. Eng.*, **33**, 997 (2016).
3. S. P. Ravi, K. Cheedrala and M. S. Diallo, *J. Nanopart. Res.*, **14**, 884 (2012).
4. T. A. Otitoju, A. L. Ahmad and B. S. Ooi, *J. Water Process Eng.*, **14**, 41 (2016).
5. D. Khojasteh, M. Kazerooni, S. Salarian and R. Kamali, *J. Ind. Eng. Chem.*, **42**, 1 (2016).
6. F. Tasselli and E. Drioli, *J. Memb. Sci.*, **301**, 11 (2007).
7. T. A. Otitoju, A. L. Ahmad and B. S. Ooi, *J. Ind. Eng. Chem.*, **47**, 19 (2017).
8. M. Khayet, C. Y. Feng and T. Matsuura, *J. Membr. Sci.*, **213**, 159 (2003).
9. M. Li, M. Liu, Y. Xu and Y. Qin, *Fibers Polym.*, **14**, 616 (2013).
10. B. P. Ter Meulen, *Basic Principles of Membrane Technology*, Recl des Trav Chim des Pays-Bas, Dordrecht (1992).
11. X. Tan, N. Liu, B. Meng and S. Liu, *J. Membr. Sci.*, **378**, 308 (2011).
12. W. Yin, B. Meng, X. Meng and X. Tan, J. *Alloys Compd.*, **476**, 566 (2009).
13. Z. Wang, N. Yang and B. Meng, *Ind. Eng. Chem. Res.*, **48**, 510 (2009).
14. B. Zydorczak, Z. Wu and K. Li, *Chem. Eng. Sci.*, **64**, 4383 (2009).
15. A. Salahi, T. Mohammadi, R. M. Behbahani and M. Hemmati, *Korean J. Chem. Eng.*, **32**, 1101 (2015).
16. G. Bakeri, M. Rezaei-Dashtarzhandi and A. Fauzi Ismail, *Korean J. Chem. Eng.*, **34**, 160 (2017).
17. C. H. Loh and R. Wang, *J. Membr. Sci.*, **466**, 130 (2014).
18. P. Z. Çulfaz, M. Wessling and R. G. H. Lammertink, *J. Membr. Sci.*, **369**, 221 (2011).
19. S. Bonyadi, T. S. Chung and W. B. Krantz, *J. Membr. Sci.*, **299**, 200 (2007).
20. A. F. Ismail, M. I. Mustaffar, R. M. Illias and M. S. Abdullah, *Sep. Purif. Technol.*, **49**, 10 (2006).
21. L. Shi, R. Wang and Y. Cao, *J. Membr. Sci.*, **305**, 215 (2007).
22. X. Li, H. Liu and C. Xiao, *J. Appl. Polym. Sci.*, **128**, 1054 (2013).
23. A. Idris, A. F. Ismail, M. Y. Noordin and S. J. Shilton, *J. Membr. Sci.*, **205**, 223 (2002).
24. F. Tasselli, J. C. Jansen, F. Sidari and E. Drioli, *J. Membr. Sci.*, **255**, 13 (2005).
25. Y. Liu, G. H. Koops and H. Strathmann, *J. Membr. Sci.*, **223**, 187 (2003).
26. R. C. Ruaan, H. L. Chou, H. A. Tsai and J. Y. Lai, *J. Membr. Sci.*, **190**, 135 (2001).
27. S. Yang and Z. Liu, *J. Membr. Sci.*, **222**, 87 (2003).
28. Z. K. Xu, L. Q. Shen and Q. Yang, *J. Membr. Sci.*, **223**, 105 (2003).
29. T. Liu, S. Xu and D. Zhang, *Desalination*, **85**, 1 (1991).
30. Y. Peng, Y. Dong and H. Fan, *DES.*, **316**, 53 (2013).
31. P. Praveen, D. Thi, T. Nguyen and K. Loh, *Biochem. Eng. J.*, **94**, 125 (2015).
32. S. A. McKelvey, D. T. Clausi and W. J. Koros, *J. Membr. Sci.*, **124**, 223 (1997).
33. F. Tasselli, J. C. Jansen and E. Drioli, *J. Appl. Polym. Sci.*, **91**, 841 (2004).
34. A. Razmjou, A. Resosudarmo and R. L. Holmes, *Desalination*, **287**, 271 (2012).
35. A. Mansourizadeh and A. R. Pouranfard, *Chem. Eng. Res. Des.*, **92**, 181 (2014).
36. S. C. Pesek and W. J. Koros, *J. Membr. Sci.*, **88**, 1 (1994).
37. S. Doi and K. Hamanaka, *Desalination*, **80**, 167 (1991).
38. J. J. Shieh and T. S. Chung, *J. Membr. Sci.*, **140**, 67 (1998).
39. S. Doi and K. Hamanaka, *Desalination*, **80**, 167 (1991).
40. X. Yang, L. Zhu and Y. Chen, *Appl. Surf. Sci.*, **349**, 916 (2015).
41. J. Qin and T. S. Chung, *J. Membr. Sci.*, **157**, 35 (1999).
42. X. Zhu, Z. Zhang and B. Ge, *J. Colloid Interface Sci.*, **432**, 105 (2014).
43. E. Fontananova, J. C. Jansen and A. Cristiano, *Desalination*, **192**, 190 (2006).
44. L. Y. Susan, S. Ismail, B. S. Ooi and H. Mustapa, *J. Water Process Eng.*, **15**, 55 (2016).
45. X. S. Yi, S. L. Yu and W. X. Shi, *Desalination*, **319**, 38 (2013).